Hindawi
International Journal of Geophysics
Volume 2022, Article ID 6171529, 10 pages
https://doi.org/10.1155/2022/6171529

Research Article

Ambient Noise H/V Spectral Ratio in Site Effect Estimation in La Mesa de Macaracas, Panama

José Ladrón De Guevara,[1] Alexis Mojica,[2,3] Alberto Ruíz,[4] Carlos A. Ho,[2] Kenia Rodríguez,[5] Jaime Toral,[6] and José Fábrega[3,7]

[1]*Facultad de Ciencias y Tecnología, Universidad Tecnológica de Panamá, 0819-07289 El Dorado, Panamá, Panama*
[2]*Laboratorio de Investigación en Ingeniería y Ciencias Aplicadas, Centro Experimental de Ingeniería, Universidad Tecnológica de Panamá, 0819-07289 El Dorado, Panamá, Panama*
[3]*Sistema Nacional de Investigación (SNI), Secretaría Nacional de Ciencia y Tecnología (SENACYT), 0816-02852 Panamá, Panama*
[4]*Fundación INDICRI, 0739 La Villa de los Santos, Panama*
[5]*Departamento de Física, Universidad de Panamá, Estafeta Universitaria, Panama*
[6]*Universidad Nacional Autónoma de Chiriquí, Ciudad Universitaria, El Cabrero, David, Panama*
[7]*Centro de Investigaciones Hidráulicas e Hidrotécnicas, Universidad Tecnológica de Panamá, 0819-07289 Panamá, Panama*

Correspondence should be addressed to Alexis Mojica; alexis.mojica@utp.ac.pa

Received 29 October 2021; Revised 15 January 2022; Accepted 5 March 2022; Published 29 March 2022

Academic Editor: Veronica Pazzi

In the last 10 years, the community of La Mesa de Macaracas (central Panama) has experienced considerable aftershocks due to earthquakes of magnitudes up to 5.7 Mw. Although most of the community consists of single-storey houses, the agricultural development in the region has led to multistorey building projects. To determine whether the characteristics of the soils could affect future construction in the study area, 16 stations were established to measure ambient vibrations and estimate the predominant frequencies and their corresponding H/V ratio peaks through the ambient noise H/V spectral ratio technique. According to the site class established by the Japan Road Association, the results revealed the existence of (a) soft soil with a range of predominant frequencies between 0.7 and 1.6 Hz, (b) medium soil with a range of predominant frequencies between 2.1 and 2.4 Hz, and (c) hard soil with a range of predominant frequencies between 2.6 and 2.9 Hz. In the first type (soft), the resonance effect could affect constructions of between 6 and 14 storeys with H/V ratio peak values (amplification factor) in the range of 2.1 and 4.3, while in the second and third types (medium and hard soils), buildings of between 3 and 5 storeys could be affected, with H/V ratio peak values (1.5–2.0) except at the SS-9 station. These results were complemented with the $V_s(30)$ values obtained in four seismic soundings carried out at the site.

1. Introduction

Mitigating seismic risk is a process closely related to site effect estimation, which can be performed by analyzing the vibrations generated by earthquakes, the impact of falling weights, or blasting [1]. However, this methodology can be time-consuming and costly, but the horizontal-to-vertical spectral analysis of ambient noise (or H/V spectral ratio) can be the key to understanding the seismic site effects in urban and semiurban or rural environments. Ambient noise also known as microtremors, refers to low-amplitude and short-period vibrations as an effect of the coasts, atmospheric loads, and wind interactions with structures and vegetation, industrial machinery, and traffic, for example. Interest in the details related to the study of soil stiffness and the interaction between buildings and soil in the predominant frequency (seismic response) was initially expressed by Nogoshi and Igarashi [2], who made numerous contributions in the use of surface waves, based on the study of the transfer function or H/V spectral ratio. Subsequently,

Table 1: Site class definition used in this project [16, 17] and the approximately corresponding NEHRP site class [18].

Site class	Site natural period (s)	Predominant frequency f_0 (Hz)	$V_s(30)$ (m/s)	NEHRP class
SC I: rock/stiff soil	$T_G < 0.2$	$f_0 > 5$	$V_{30} > 600$	A+B
SC II: hard soil	$0.2 \le T_G < 0.4$	$2.5 < f_0 \le 5$	$300 < V_{30} \le 600$	C
SC III: medium soil	$0.4 \le T_G < 0.6$	$1.6 < f_0 \le 2.5$	$200 < V_{30} \le 300$	D
SC IV: soft soil	$T_G \ge 0.6$	$f_0 \le 1.6$	$V_{30} \le 200$	E

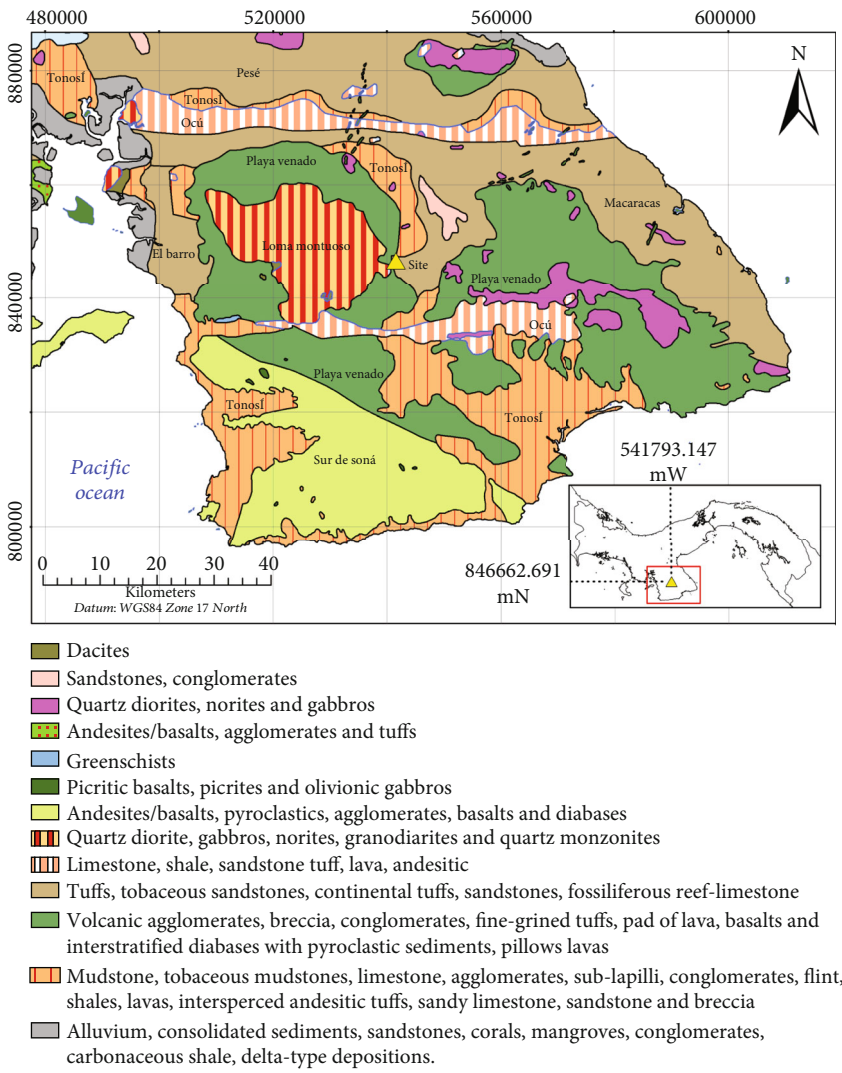

Figure 1: Generalized geological map of the site of interest and surrounding areas. Source: Geological Map of the Republic of Panama, Tommy Guardia National Geographic Institute.

Nakamura [3] defined a theoretical framework of the method that could calculate the basement depth and a vulnerability index of the surface terrain to estimate the damage an earthquake can cause to structures. At the beginning of the last century, Omori [4] discovered the presence of vibrations caused not by earthquakes but due to natural or artificial sources with amplitudes varying between 0.1 and 1.0 microns; later, Kanai and Tanaka [5] applied this concept to determine the dynamic behavior of soil. Finally, Horike [6] postulated that the vertical component of these microtremors basically consists of Rayleigh waves. Currently, several studies demonstrate the feasibility of using this type of technique for the estimation of the site response. Panou et al. [1, 7–10] have applied this technique to study the seismic risk in various areas.

In our country, in recent years, numerous efforts have been made to develop studies in this area, which increase knowledge and contribute to decision-making on policies

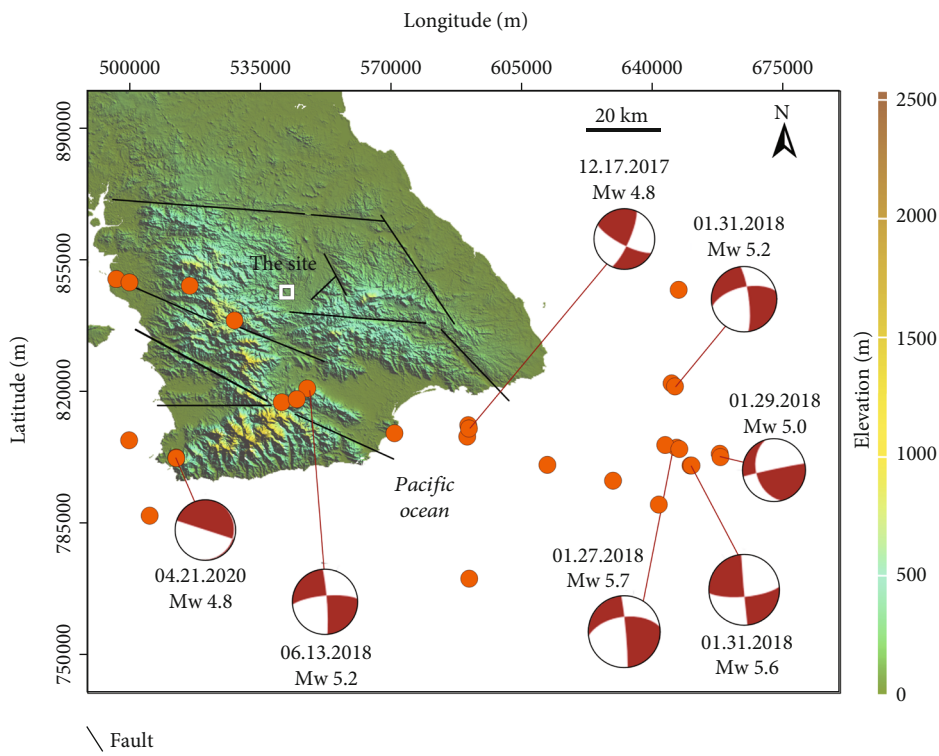

Figure 2: Recent seismicity (>4.0 Mw) and focal mechanisms in the Azuero Peninsula and its surroundings. The spatial distribution of the epicenters is represented by the orange points.

regarding risk and the type of buildings in a given area so that structures are prepared for earthquakes of considerable magnitude. For example, Echeverría [11] used the Nakamura technique to microzone the city of Puerto Armuelles. Furthermore, studies such as those conducted by Toral et al. [12–15] apply this technique to the study of seismic hazards and risks in Panama.

This research arises from the need to improve the scientific and technical knowledge base regarding the risk to buildings in the soils of our country and aims to study and determine the soil class according to the site class definition [16, 17] and the approximately corresponding NEHRP site class (see Table 1) and to estimate the potential risk to future buildings built in the region of La Mesa de Macaracas, Los Santos Province, using the ambient noise H/V spectral ratio method.

2. Geological and Seismic Context of the Area

La Mesa de Macaracas is located in the center of the Azuero Peninsula, Los Santos Province, in the central region of the Isthmus of Panama (see Figure 1). The geological conditions are strongly influenced by the tectonic processes that produced the emergence and consolidation of the Isthmus of Panama. Therefore, in this sector we note a variety of effusive, fragmentary, and intrusive rock products of complex movements and differential displacements originating from the oceanic crust of Nazca and Coco, in addition to the orogenic processes evolving since the beginning of the Cretaceous.

The study area and surroundings are characterized by the geological formations shown in Figure 1. According to the Geological Map of Panama, igneous and sedimentary rocks emerged in the investigated area, whose formation ages comprise a wide time interval (83.6 to 13.8 Myr) [19]. The study area (La Mesa de Macaracas) is located on the Macaracas Formation, which is composed of tuffs and tuffaceous sandstones.

These general conditions of the site are affected by local faults, which have deformed the surface and left traces that are currently evident in the topography and in a large part of the main and secondary surface riverbeds. Therefore, geological-tectonic events during the Eocene and Early Oligocene gave way to volcanic processes that consolidated the aforementioned formations during the Late Oligocene. Epeirogenic processes affected the La Villa River basin, as well as the regional morphology and elevations of the area. The surface at the La Mesa de Macaracas site presents a high degree of weathering and components of sandy clays that retain the surface moisture of water in the vadose zone given the poor compaction of these sediments. The PEE-3 borehole well shown in Figure 2 reveals an unconsolidated stratigraphic sedimentary sequence. Within its components, granular fractions and fragments of silicified and mineralized rocks predominate. These subrounded fragments in combination with sandy and clayey material suggest the existence of a paleochannel, as these types of subrounded fragmentary rocks and their levels

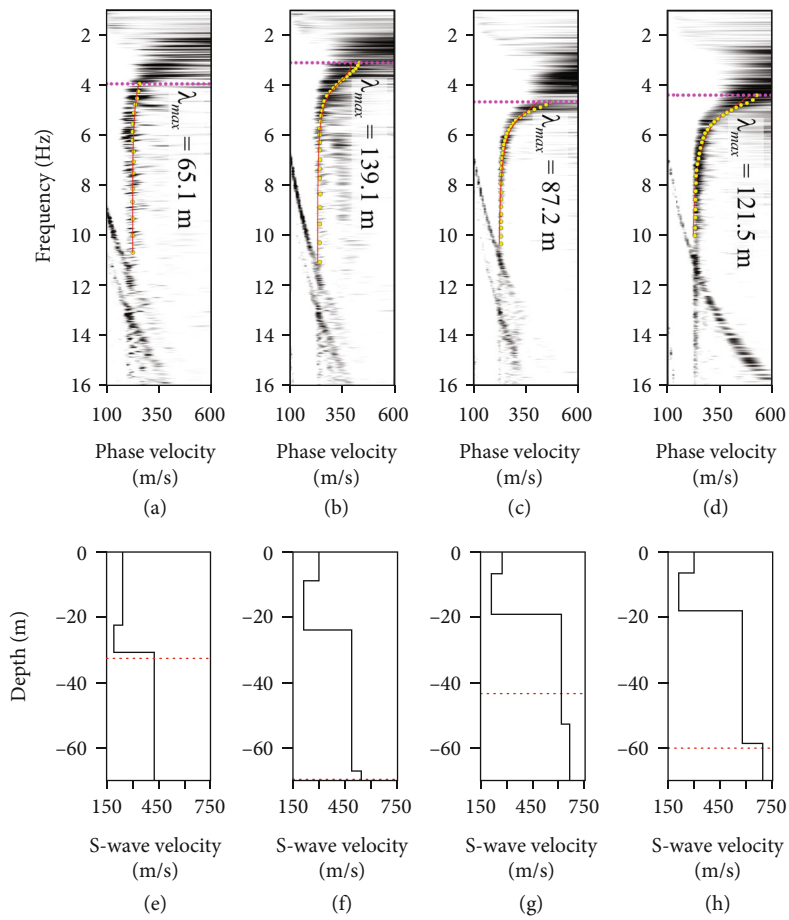

Figure 3: Stacked dispersion images and curves obtained for ReMi-1, 2, 3, and 4 sounding (a, b, c, and d, respectively) and 1D inversion results obtained for each dispersion curve of ReMi-1, 2, 3, and 4 soundings (e, f, g, and h, respectively). The yellow circles correspond to observations, the continuous red line is the model response, and the red dashed lines in 1D models are the DOI (depth of investigation).

Table 2: Dynamic soil parameters and match values between the observations and model response obtained from the inversion process for each seismic sounding.

Sounding	$V_s(30)$ m/s	DOI (m)	Dispersion curve match (%)
ReMi-1	226	32.6	97.8
ReMi-2	261	69.6	94.1
ReMi-3	290	43.6	93.4
ReMi-4	301	60.8	94.5

of hydrothermal alteration coincide with eroded mineralized outcrops located in the upper channels of the La Villa River, which were possibly washed away during epeirogenic processes in the Late Oligocene. Some 1D and 2D geophysical studies developed at the site corroborate the existence of this type of geological structure [20].

The area of La Mesa de Macaracas is seismically active and consists of various geological faults and would also be on the subduction interface plane between the Nazca plate and the Panama microplate. According to Bunduschuh and Alvarado [21] in Azuero, a system of active left-lateral strike-slip faults run in an NW-SE direction [22–24]. One of the most significant events close to the site was that on June 13, 2018, with a magnitude (Mw) of 5.2 and a dextral focal mechanism with an approximate east-west orientation, which is the characteristic of that region (see the focal mechanism of Figure 2).

3. $V_s(30)$ Classification

At the study site, four seismic soundings (ReMi-1, 2, 3, and 4) were previously developed using the refraction microtremor method (ReMi survey) or multichannel analysis of surface waves [25], which permit the estimation of the S-wave velocity of subsoil through the study of surface waves. These soundings were separated by a distance of 117.5 m in a southwest–northeast direction (see Figure 3), where the average shear wave velocity for the top 30 m of soil ($V_s(30)$) values was obtained. These values were used to complement the results obtained in the ambient noise H/V spectral ratio in the site. For each sounding, 20 natural noise files were recorded using 16 low-frequency geophones with a geophone spacing of 10 m. For the generation of the dispersion images, the extraction of dispersion curves, and the inversion process, the ParkSEIS software was used. The results are shown in Figure 3.

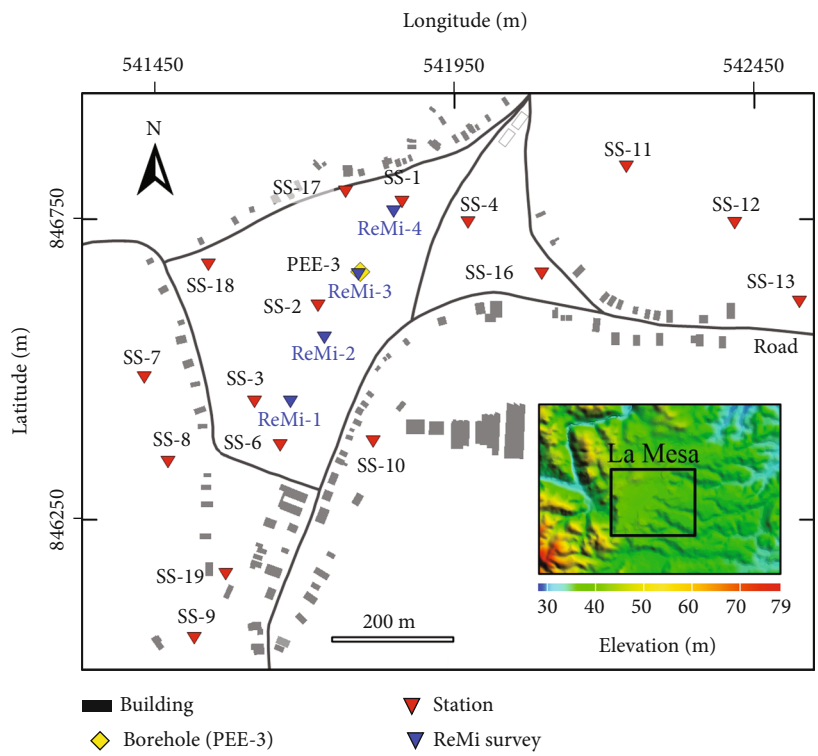

Figure 4: Distribution of the 16 ambient noise recording stations, civil structures, seismic soundings (ReMi), and streets in La Mesa de Macaracas, Province of Los Santos.

The $V_s(30)$ values, the dispersion curve match, and the depth of investigation (DOI) are summarized in Table 2.

4. H/V Spectral Ratio Technique

The H/V spectral ratio technique, also known as the Nakamura method, is based on a few assumptions, including the hypotheses that the energy of a microtremor consists mainly of Rayleigh-type surface waves and that the amplification effect of the site is due to the presence of a layer of soil on the surface that rests on a rocky mantle. Under these conditions, the amplitude spectra of four motion components are considered: two horizontal motion components recorded on the surface $H_s(f)$ and in the rock $H_b(f)$, and two vertical motion components recorded on the surface $V_s(f)$ and in the rock $V_b(f)$. From this, two important parameters can be defined: the first is related to the amplitude effect of the source through the $V_s(f)/V_b(f)$ ratio, and the second is linked to the site effects through the $H_s(f)/H_b(f)$ ratio [3]. From these, a modified site effect function $S_M(f)$ is defined to compensate for the effect of the source. The ratio between the site effects and the amplitude effect of the source represents this function. If it is assumed that the horizontal and vertical movements in the rock are equal, then the ratio $H_b(f)/V_b(f) = 1$, and the modified function is expressed as follows:

$$S_M(f) = \frac{H_s(f)}{V_s(f)}. \quad (1)$$

Equation (1) is also known as the Nakamura ratio.

5. Methodology

The present study was performed by collecting ambient noise data from 16 stations distributed in La Mesa de Macaracas (see Figure 4); these measurements were performed on December 10 and 11, 2020, which correspond to the beginning of the dry season in the Panamanian tropics where weather conditions are suitable. A portable seismograph GEOtiny (from GEObit) was used in which the sampling frequency was established at 100 Hz in a wide dynamic range with a root mean square (RMS) of 129 dB. At each station, the seismograph was aligned to the north and covered with a box to prevent wind effects. The recorded data were displayed on a laptop using SeisGram2K software and stored on the seismograph; a record length of 20 minutes was established at each station, noting the very low anthropic activity and its possible negative influence on the H/V ratio peaks; therefore, the measurements can be considered stratigraphic.

Ambient noise records were processed using the winMASW software (of Eliosoft) in two main steps:. (1) The transient events present in the raw data of each channel were removed (i.e., raw data obtained in station SS-10, Figure 5(a)) through rectangles or windows that highlight them. A baseline correction is performed, and the data

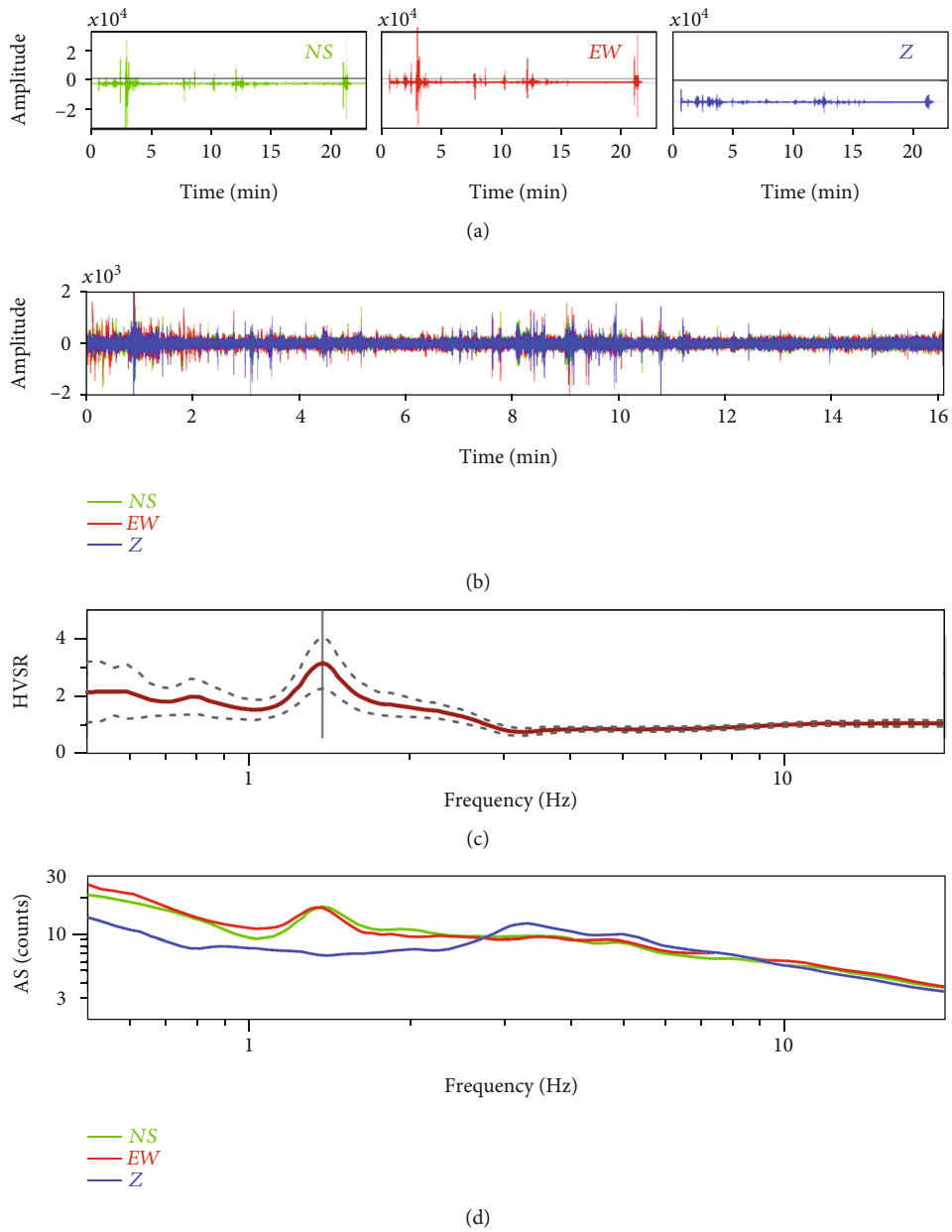

Figure 5: (a) Raw signals of ambient noise in the three components obtained at the SS-10 station. (b) Result of the removal of transient events, analysis of the amplitude thresholds and the H/V spectral ratio, and adjustment to baseline. (c) Graph of the H/V spectral ratio as a function of frequency as a result of the Nakamura analysis with maximum and minimum values (gray dotted lines), with a continuous gray vertical line that represents the predominant frequency of the soil. (d) Average spectra (AS) obtained for each component.

of the three components are displayed in the same graph as shown in Figure 5(b). (2) The three fundamental parameters were defined: window length, spectral smoothing, and tapering [26]. Moving this window (which can be a function of frequencies associated with H/V ratio peak values of interest) allows the H/V spectral ratio to be computed for all considered windows or segments. The spectral smoothing can be relevant for the predominance of lower frequencies, and the tapering parameter is fixed to avoid artifacts during the computation of Fourier spectra [26]. Figures 5(c) and 5(d) illustrate the average of all computed H/V spectral ratio curves and the standard deviations, and the average spectra for each component, respectively. These operations are based on the SESAME criteria [27].

In Figure 5(c), the predominant frequency obtained from the H/V ratio peak curve coincides with the eye-shaped detachment in the average spectral curves of Figure 5(d), which means that the peaks are stratigraphic and not anthropic or artificial. These sources mainly affect the vertical component of the movement and therefore tend to induce Rayleigh waves [3].

Table 3: Information on the 16 stations established for the acquisition of ambient noise data with the corresponding predominant frequencies and H/V ratio peaks.

Station	Geographic coordinates UTM (m)		Predominant frequency f_0 (Hz)	H/V ratio peaks
SS-1	541862	846778	2.6	1.8
SS-2	541722	846606	2.4	1.8
SS-3	541617	846446	1.4	2.4
SS-4	541972	846744	2.3	1.9
SS-6	541659	846373	1.4	2.3
SS-7	541433	846486	1.6	2.1
SS-8	541472	846346	1.6	2.4
SS-9	541516	846053	2.2	2.5
SS-10	541814	846380	1.4	3.1
SS-11	542236	846837	1.2	3.6
SS-12	542417	846743	1.0	3.4
SS-13	542525	846612	2.1	1.5
SS-16	542095	846659	2.9	1.8
SS-17	541768	846795	2.6	2.0
SS-18	541539	846674	0.7	4.3
SS-19	541568	846159	1.0	2.8

6. Results

The Resulting Dataset Is Characterized by the Position (x, y) of Each Station (in UTM Coordinates) and the Predominant Frequency (in Hz) Obtained from the H/V Ratio Peak (See Table 3).

6.1. Classification of H/V Spectral Ratios. Noting the shape of the graphs of the H/V spectral ratio versus the frequency and the H/V ratio peaks recorded in Table 3, two classes of spectral ratios are defined:

(i) Class I: spectral ratios with a moderately marked peak and H/V ratio peaks that vary between 1.5 and 2.0

(ii) Class II: spectral ratios with a well-marked peak and H/V ratio peaks between 2.1 and 4.3

This type of classification of H/V spectral ratios was proposed by Pastén [28]. Figure 6 presents two examples of the maximum frequency pulses obtained at stations SS-1 and SS-10.

6.2. Spatial Distribution of the Predominant Frequencies and H/V Ratio Peaks. The spatial distributions of the predominant frequencies and H/V ratio peaks were obtained using Surfer 19 software (Golden Software); these datasets were interpolated through kriging as an accurate gridding method, which is adapted in this software. Figure 7(a) shows the interpolated map of the predominant frequencies of the soils in the study site with the site classes defined in Table 1 (see predominant frequency limits in the color bar of this map).

Based on the classification of the H/V spectral ratios established at the previous point, a second interpolated map of H/V ratio peaks was developed (see Figure 7(b)). Figure 7(c) shows the spatial distribution of the georeferenced stations whose soils correspond to classes I and II.

7. Discussion

In the map in Figure 7(a), it is possible to identify the following zones:

(i) The first zone is represented by tuft blue and pale golden tones and characterized by the lower range of predominant frequency values (0.7 to 1.6 Hz). According to the literature, this range suggests soft soils in the eastern, western, and southwestern ends of the study area

(ii) The second zone is located in the north-central part of the site and represented by flavescent and brick red tones. The range of predominant frequency values of this zone oscillates between 2.1 and 2.9 Hz; this range suggests medium and hard soil

In the first zone is a seismic survey (ReMi-1) with a low value of $V_s(30)$ (226 m/s); this value can be associated with the transition zone between the soft and medium soils. In the second zone are the following three seismic surveys (ReMi-2, 3, and 4), with $V_s(30)$ values of 261, 290, and 301 m/s in which the first two are associated with medium soil and the last sounding with hard soil. These are complemented by the results of the predominant frequencies obtained in this study for the site classification.

The predominant frequency and the $V_s(30)$ values obtained show an increase towards the central north of the site. This could be associated with the fact that the soils are more consolidated in this area compared to the surroundings, according to the PEE-3 borehole and others carried out near of the site.

In the maps of Figures 7(b) and 7(c), two zones can be identified, which according to the ranges of the H/V ratio peaks (classification established by spectral ratio) are as follows:

(i) The class I zone is represented by green tones with a range of the H/V ratio peaks between 1.5 and 2.0. This zone is located in the north-central sector of the study area

(ii) The class II zone is represented by yellow and orange tones with a range of H/V ratio peaks between 2.1 and 4.3. This zone occupies a large part of the study area, extending to the eastern, western, and southwestern ends of the site

The spatial distributions of the predominant frequency and the H/V ratio peak values represented in the maps of Figure 7 appear to be partially related, as the zone of low predominant frequencies of the soil appears to be associated with the class II zone which presents high H/V ratio peak values (amplification effect), and according to Bodare [29],

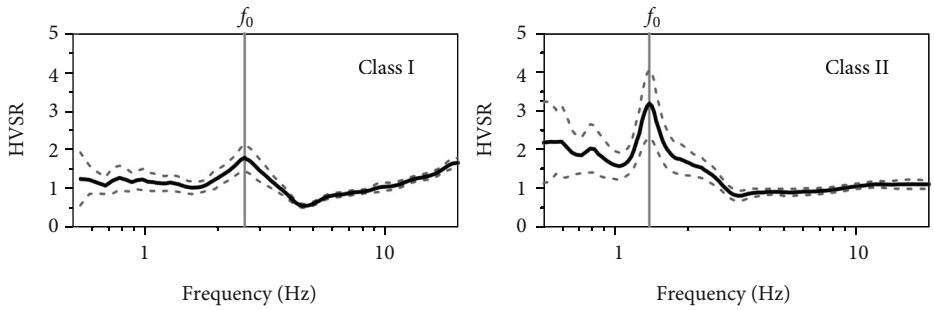

Figure 6: Examples of the H/V spectral ratio classes obtained at stations SS-1 (class I) located in the northern area and SS-10 (class II) located in the central sector of the study area.

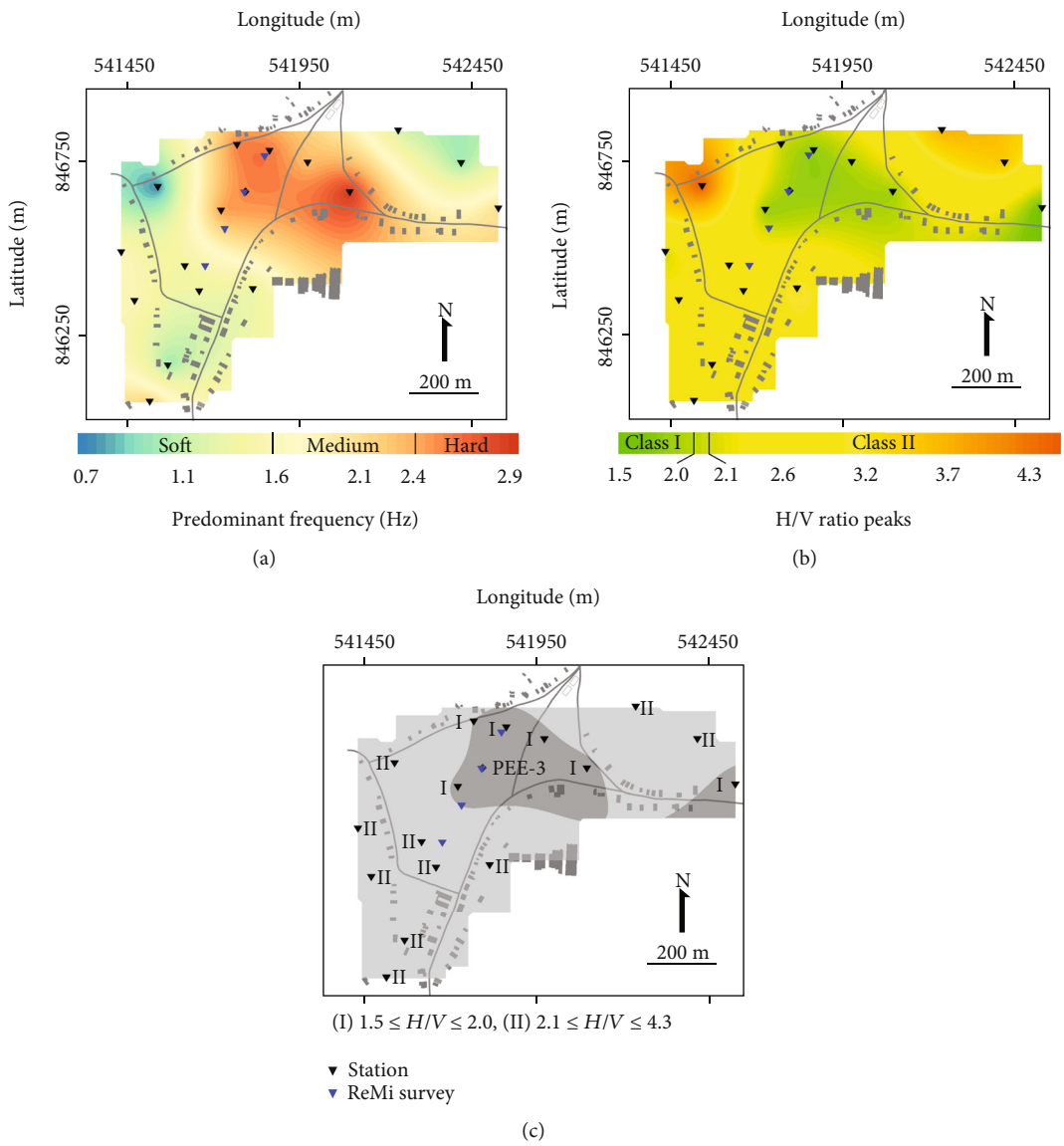

Figure 7: Interpolated maps that represent (a) the predominant frequencies of the soil, (b) the H/V ratio peaks, and (c) the classification of the soils according to these H/V ratio peaks.

from the structural perspective of buildings and based on these field results, we can empirically establish that this zone would shake most strongly the constructions ranging between 6 and 14 storeys. This zone can be classified as soft soils. The north-central zone characterized by a higher range of predominant frequencies seems to be associated with the class I zone, which has lower H/V ratio peak values, which agrees with medium and hard soils and could affect buildings with between 3 and 5 storeys.

There is an exception at the SS-9 station at the southwest end of the study area, where the predominant frequency suggests the existence of medium soil, but the H/V ratio peak value is associated with soft soil (class II zone). This exception could be associated with the size and distribution of the pebbles identified in the surface layer of the site through a borehole established in the southern part.

8. Conclusions

The validity of the estimation of the seismic response characteristic of the ambient noise measurements was investigated in La Mesa de Macaracas, Province of Los Santos, central sector of the Isthmus of Panama. The spatial distributions of predominant frequencies and the H/V ratio peaks of the soils suggest the existence of soft, medium, and hard soils in the study area. The range of predominant frequency obtained in this study (0.7–2.9 Hz) could be associated with a set of unconsolidated sedimentary sequences formed by subrounded alluvial fragments, sandy material, and clays with a thickness that could exceed 50 m. Two zones were clearly identified: the class I zone, with higher predominant frequency values (medium and hard soils) and lower spectral ratio values (low amplification), and the class II zone, characterized by a lower predominant frequency range (soft soil) and higher spectral ratio values (high amplification). Therefore, resonance could affect constructions that comprise 3 to 5 storeys in medium and hard soils and between 6 and 14 storeys in soft soils. For this type of geological environment, it is important to consider these results, noting the construction materials and minimum requirements established in the current structural regulations, thus ensuring that these civil works are not affected by significant seismic events. The classification developed in this work can be considered very useful for the structural analysis of new construction, since buildings or structures built on soft, medium, or hard soils could be affected by seismic amplification.

Data Availability

The data that supports this research is in the private database of the Centro Experimental de Ingeniería of the Universidad Tecnológica de Panamá, where special permits are required by the corresponding university authorities (contact by mail: alexis.mojica@utp.ac.pa).

Conflicts of Interest

The authors declare that there is no conflict of interest regarding the publication of this paper.

Acknowledgments

The authors would like to thank the SENACYT and the Sistema Nacional de Investigación (SNI) for all their support. We would also like to thank the Laboratorio de Investigación en Ingeniería y Ciencias Aplicadas of the Centro Experimental de Ingeniería at the Universidad Tecnológica de Panamá for their valuable logistical support. This work was supported by the Secretaría Nacional de Ciencia, Tecnología e Innovación (SENACYT in Spanish) (grant number APY-NI-2029A-06).

References

[1] A. Panou, N. Theodoulidis, and K. Stylianidis, "Ambient noise horizontal-to-vertical spectral ratio in site effects estimation and correlation with seismic damage distribution in urban environment: the case of the city of Thessaloniki (Northern Greece)," *Soil Dynamics and Earthquake Engineering*, vol. 25, no. 4, pp. 261–274, 2005.

[2] M. Nogoshi and T. Igarashi, "On the amplitude characteristics of microtremor (part 2)," *Journal of the Seismological Society of Japan*, vol. 24, pp. 26–40, 1971.

[3] Y. Nakamura, "A method of dynamic characteristics estimation of subsurface using microtremor on the ground surface," *Railway Technical Research Institute, Quarterly Reports*, vol. 30, no. 1, pp. 25–33, 1989.

[4] F. Omori, "Preliminary note on the Formosa Earthquake of March 17, 1906," *Bulletin of the Imperial Earthquake Investigation Committee*, vol. 1, no. 2, pp. 53–69, 1907.

[5] K. Kanai and T. Tanaka, "Observations of the earthquake motion at the different depths of the earth, part I," *Bulletin of Earthquake Research Institute*, vol. 29, no. article 29, pp. 107–113, 1951.

[6] M. Horike, "Inversion of phase velocity of long-period microtremors to the S-wave-velocity structure down to the basement in urbanized areas," *Journal of Physics of the Earth*, vol. 33, no. 2, pp. 59–96, 1985.

[7] R. Franklin, J. O. Caselles Magallón, J. A. Canas Torres et al., "Estimación de la respuesta de sitio mediante el método del cociente espectral aplicado a ruido ambiental: aplicación a la Ciutat Vella de Valencia," *Revista Internacional de Métodos Numéricos para Cálculo y Diseño en Ingeniería*, vol. 22, no. 2, pp. 169–192, 2006.

[8] R. Ritta, L. Suárez, and M. Pando, "Determinación del período fundamental del suelo usando vibración y el cociente espectral horizontal/vertical," *Mecánica Computacional*, vol. 31, no. 8, pp. 1399–1419, 2012.

[9] S. M. Talha Qadri, B. Nawaz, S. H. Sajjad, and R. A. Sheikh, "Ambient noise H/V spectral ratio in site effects estimation in Fateh Jang area, Pakistan," *Earthquake Science*, vol. 28, no. 1, pp. 87–95, 2015.

[10] L. Vargas and R. Verdugo, "Características del terreno de fundación de sitios con edificios dañados severamente en el terremoto del 27F," *Obras y Proyectos*, vol. 21, no. 21, pp. 46–53, 2017.

[11] Y. Echeverría, *Microzonificación sísmica de la Ciudad de Puerto Armuelles mediante la Técnica de Nakamura Provincia de Chiriquí, Panamá*, Instituto de Geociencias UP, Panama, 2011.

[12] J. Toral, C. A. Ho, C. Lindholm, A. Tapia, and E. Chichaco, *Amplificación Sísmica de los Suelos de David Chiriquí*, Capítulo V de la Microzonificación Sísmica de David, Report, Instituto de Geociencias UP, NGI, NORSAR and CEPRE-DENAC, 2000.

[13] A. Hedlund and S. Sivars, *Microzonation study in David, Panama*, Royal Institute of Technology, Sweden, 1999.

[14] E. Pettersen, *Microzonation study in La Chorrera, Panama*, Royal Institute of Technology, Sweden, 2001.

[15] M. Aizprúa and D. Toral, *Utilización del método de Nakamura y la tomografía de resistividad eléctrica para la caracterización de los suelos y la detección de fallas geológicas en el sector de Panamá Pacífico*, Facultad de Ingeniería Civil, Universidad Tecnológica de Panamá, Panama, 2019.

[16] Japan Road Association, *Specifications for Highway Bridges Part V*, Maruzen Co., LTD., Seismic Design, 1980.

[17] Japan Road Association, *Specifications for Highway Bridges Part V*, Maruzen Co., LTD., Seismic Design, 1990.

[18] Building Seismic Safety Council (BSSC), "The 2000 NEHRP Recommended Provisions for New Buildings and Other Structures," *Part I (Provisions) and Part II (Commentary)*, vol. 368, article 369, 2000.

[19] V. Opolenko, "Identificación y caracterización de potenciales sistemas acuíferos en la parte media y baja de la cuenca del río La Villa, República de Panamá," *Revista Geográfica de América Central*, vol. 2, no. 67, pp. 109–146, 2021.

[20] F. Rejiba, A. Mojica, M. Schmutz et al., "Geophysical characterization of near-surface formations in the La Villa River catchment (Los Santos, Panama)," *NSG2021 1st Conference on Hydrogeophysics*, vol. 2021, no. 1, pp. 1–5, 2021.

[21] J. Bunduschuh and G. E. Alvarado, *Central America: Geology, Resources, Hazards*, vol. 1, CRC Press, Taylor & Francis, USA, 2007.

[22] N. C. Hardy, R. P. Heath, and G. K. Westbrook, "A complex plate boundary south of the Gulf of Panama," *EOS Transactions of the American Geophysical Union*, vol. 71, article 1593, 1990.

[23] R. A. Kolarsky and P. Mann, "Structure and neotectonics of an oblique-subduction margin, southwestern Panama," in *Geologic and Tectonic Development of the Caribbean Plate Boundary in Southern Central America, Geological Society of America*, pp. 131–157, Special Papers-Geological Society Of America, USA, 1995.

[24] D. M. Buchs, R. J. Arculus, P. O. Baumgartner, C. Baumgartner-Mora, and A. Ulianov, "Late Cretaceous arc development on the SW margin of the Caribbean Plate: insights from the Golfito, Costa Rica, and Azuero, Panama, complexes," *Geochemistry, Geophysics, Geosystems*, vol. 11, no. 7, pp. 1–35, 2010.

[25] C. B. Park, R. D. Miller, and J. Xia, "Multichannel analysis of surface waves," *Geophysics*, vol. 64, no. 3, pp. 800–808, 1999.

[26] G. Dal Moro, *Surface Wave Analysis for Near Surface Applications*, Elsevier, Netherlands, 2015.

[27] C. Acerra, G. Aguacil, A. Anastasiadis et al., "Guidelines for the implementation of the H/V spectral ratio technique on ambient vibrations: measurements, processing and interpretation," in *No. European Commission–EVG1-CT-2000-00026 SESAME*, European Commission. Project, Brussels, Belgium, 2004.

[28] C. Pastén, *Respuesta Sísmica de la cuenca de Santiago*, University of Chile, Chile, 2007.

[29] A. Bodare, *Jord-Och Bergdynamik. Division of Soil and Rock*, Royal Institute of Technology, Stockholm, Sweden, 1997.